blood®
Regular Article

IMMUNOBIOLOGY AND IMMUNOTHERAPY

Immunogenomic identification and characterization of granulocytic myeloid-derived suppressor cells in multiple myeloma

Cristina Perez,[1,*] Cirino Botta,[1,2,*] Aintzane Zabaleta,[1] Noemi Puig,[3] Maria-Teresa Cedena,[4] Ibai Goicoechea,[1] Daniel Alameda,[1] Edurne San José-Eneriz,[1] Juana Merino,[1] Paula Rodríguez-Otero,[1] Catarina Maia,[1] Diego Alignani,[1] Patricia Maiso,[1] Irene Manrique,[1] David Lara-Astiaso,[1] Amaia Vilas-Zornoza,[1] Sarai Sarvide,[1] Caterina Riillo,[5] Marco Rossi,[5] Laura Rosiñol,[6] Albert Oriol,[7] María-Jesús Blanchard,[8] Rafael Rios,[9] Anna Sureda,[10] Jesus Martin,[11] Rafael Martinez,[12] Joan Bargay,[13] Javier de la Rubia,[14,15] Miguel-Teodoro Hernandez,[16] Joaquin Martinez-Lopez,[4] Alberto Orfao,[3,17-19] Xabier Agirre,[1] Felipe Prosper,[1] Maria-Victoria Mateos,[3] Juan-José Lahuerta,[4] Joan Blade,[6] Jesús F. San-Miguel,[1] and Bruno Paiva,[1] on behalf of the Grupo Español de Mieloma/Programa para el Estudio de la Terapéutica en Hemopatías Malignas Cooperative Study Group

[1]Clinica Universidad de Navarra, Centro de Investigacion Medica Aplicada (CIMA), Instituto de Investigacion Sanitaria de Navarra (IDISNA), CIBER-ONC numbers CB16/12/00369, CB16/12/00489, Pamplona, Spain; [2]Department of Oncohematology, "Annunziata" Hospital, Cosenza, Italy; [3]Hospital Universitario de Salamanca, Instituto de Investigacion Biomedica de Salamanca (IBSAL), Centro de Investigación del Cancer (IBMCC-USAL, CSIC), CIBER-ONC number CB16/12/00233, Salamanca, Spain; [4]Hospital 12 de Octubre, CIBER-ONC number CB16/12/00369, Madrid, Spain; [5]Department of Clinical and Experimental Medicine, "Magna Graecia" University of Catanzaro, Catanzaro, Italy; [6]Hospital Clínic IDIBAPS, Barcelona, Spain; [7]Institut Català d'Oncologia i Institut Josep Carreras, Badalona, Spain; [8]Hospital Ramón y Cajal, Madrid, Spain; [9]Hospital Virgen de las Nieves, Granada, Spain; [10]Institut Català d'Oncologia-Hospitalet, Instituto de Investigación Biomédica de Bellvitge (IDIBELL), Barcelona, Spain; [11]Hospital Universitario Virgen del Rocío, Instituto de Biomedicina de Sevilla (IBIS/CSIC/CIBERONC CB16/12/00480), Seville, Spain; [12]Hospital Clínico San Carlos, Madrid, Spain; [13]Hospital Son Llatzer, Palma de Mallorca, Spain; [14]Hospital Universitario y Politécnico La Fe, Valencia, Spain; [15]School of Medicine and Dentistry, Catholic University of Valencia, Valencia, Spain; [16]Hospital Universitario de Canarias, Santa Cruz de Tenerife, Spain; [17]Cancer Research Center (IBMCC-CSIC/USAL-IBSAL), CIBER-ONC number CB16/12/00400, Salamanca, Spain; [18]Cytometry Service (NUCLEUS) and Department of Medicine, University of Salamanca, Salamanca, Spain; and [19]Centro de Investigación Biomédica en Red de Cáncer, Instituto Carlos III, Madrid, Spain

KEY POINTS

- There is a progressive gradient of immunosuppression from immature to mature neutrophils present in the myeloma microenvironment.
- $CD11b^+CD13^+CD16^+$ mature neutrophils are epigenetically deregulated, and their abundance in the myeloma microenvironment is prognostic.

Granulocytic myeloid-derived suppressor cells (G-MDSCs) promote tumor growth and immunosuppression in multiple myeloma (MM). However, their phenotype is not well established for accurate monitoring or clinical translation. We aimed to provide the phenotypic profile of G-MDSCs based on their prognostic significance in MM, immunosuppressive potential, and molecular program. The preestablished phenotype of G-MDSCs was evaluated in bone marrow samples from controls and MM patients using multidimensional flow cytometry; surprisingly, we found that $CD11b^+CD14^-CD15^+CD33^+HLADR^-$ cells overlapped with common eosinophils and neutrophils, which were not expanded in MM patients. Therefore, we relied on automated clustering to unbiasedly identify all granulocytic subsets in the tumor microenvironment: basophils, eosinophils, and immature, intermediate, and mature neutrophils. In a series of 267 newly diagnosed MM patients (GEM2012MENOS65 trial), only the frequency of mature neutrophils at diagnosis was significantly associated with patient outcome, and a high mature neutrophil/T-cell ratio resulted in inferior progression-free survival ($P < .001$). Upon fluorescence-activated cell sorting of each neutrophil subset, T-cell proliferation decreased in the presence of mature neutrophils (0.5-fold; $P = .016$), and the cytotoxic potential of T cells engaged by a BCMA×CD3-bispecific antibody increased notably with the depletion of mature neutrophils (fourfold; $P = .0007$). Most interestingly, RNA sequencing of the 3 subsets revealed that G-MDSC–related genes were specifically upregulated in mature neutrophils from MM patients vs controls because of differential chromatin accessibility. Taken together, our results establish a correlation between the clinical significance, immunosuppressive potential, and transcriptional network of well-defined neutrophil subsets, providing for the first time a set of optimal markers (CD11b/CD13/CD16) for accurate monitoring of G-MDSCs in MM. **(*Blood*. 2020;136(2):199-209)**

Introduction

Myeloid-derived suppressor cells (MDSCs) are described as a mixture of immature cells that have common biological activity. They are able to influence innate and adaptive immune responses through depletion of L-arginine, generation of oxidative stress, induction of cytotoxic T-cell apoptosis, and activation of T regulatory cells.[1] All these mechanisms lead to immune supression.[2,3]

MDSCs have been extensively studied in mice and less frequently in humans. Whereas in mice they are identified based on expression of Gr-1 and CD11b, the immunophenotype of their human counterpart remains unclear.[4] Commonly, they are defined as a $CD11b^{+}CD33^{+}HLADR^{-/lo}$ subset among mononucleated cells isolated after density gradient.[3,5] Cells with such phenotype were found to be rare in healthy adults (HAs) but expanded in patients with cancer. Two subsets of MDSCs have been identified based on the additional expression of CD14 or CD15: monocytic MDSCs and granulocytic MDSCs (G-MDSCs), respectively.[2,4-6]

In multiple myeloma (MM), malignant plasma cells colonize and modify the bone marrow (BM) microenvironment through cytokine production and bidirectional interactions with other cell types. Namely, it has been suggested that MM cells induce MDSC development and survival, whereas MDSCs promote tumor growth and induce immune suppression.[7-10] In addition, antimyeloma therapies such as dexamethasone, melphalan, or cyclophosphamide or even immunomodulatory drugs could expand and potentiate MDSC immunosuppressive effects, most likely as a counterregulatory mechanism.[8] By contrast, recent data suggest that daratumumab acts, among other modes of action, by depleting MDSCs.[6,7,11] Thus, MDSC suppression could become an important strategy for increasing and prolonging the efficacy of novel immunotherapies (eg, chimeric antigen receptor T cells or T-cell engager bispecific antibodies), but for this to be the case, precise knowledge of the phenotype of MDSCs would be required for its clinical monitoring in the MM tumor microenvironment.

Enumeration of putative G-MDSCs was shown to correlate with MM burden but never with patient survival.[12,13] However, it is challenging to dissect causal effects and mechanistic functions based solely on tumor burden. This study overcomes these limitations by integrating clinical, functional, and molecular data on granulocytic cells from the tumor microenvironment and provides a set of markers for optimal monitoring of G-MDSCs in MM.

Patients and methods

Patients and treatment

A total of 388 BM samples from 22 HAs and 366 patients with MM were analyzed in this study (median age of 54 and 64 years, respectively). Only samples with $>$ 90% viability (according to the percentage of debris identified by flow cytometry) were used for downstream analysis. Of the 366 MM patients, 267 were enrolled in the PETHEMA/GEM2012MENOS65 clinical trial (registered at www.clinicaltrials.gov as #NCT01916252), and this cohort was selected to determine the prognostic value of the distribution of various granulocytic subsets in the tumor microenvironment. Briefly, patients received 6 induction cycles of bortezomib, lenalidomide, and dexamethasone, underwent autologous stem-cell transplantation conditioned with Bu-Mel or Mel-200 high-dose therapy, and received 2 consolidation cycles of bortezomib, lenalidomide, and dexamethasone.[14] Afterward, patients were enrolled in the PETHEMA/GEM2014MAIN clinical trial (registered at www.clinicaltrials.gov as #NCT02406144), which randomized maintenance with lenalidomide plus dexamethasone or lenalidomide plus dexamethasone plus ixazomib for 2 years, after which patients continued with lenalidomide plus dexamethasone for 3 additional years if minimal residual disease positive or stopped therapy if minimal residual disease negative.[15] Median follow-up was 39 months (range, 7-57 months). The independent ethics committee at each study site approved the protocol and informed consent forms required before patient enrollment. The study was conducted per the ethical principles of the Declaration of Helsinki.

Multidimensional flow cytometry

Multidimensional flow cytometry was used to evaluate the preestablished phenotype of G-MDSCs[2,3,6-9,12,16] in BM samples from HAs (n = 7) and MM patients (n = 10), and compare their phenotype in paired BM and peripheral blood (PB) samples from MM patients (n = 5). Briefly, the EuroFlow lyse, wash, and stain standard sample preparation protocol adjusted to 10^6 nucleated cells, together with the 8-color combination of the monoclonal antibodies (mAbs) HLADR-BV421, CD45-OC515, CD15-FITC, CD13-PE, CD33-PerCPCy5.5, CD16-PECy7, CD11b-APC, and CD14-APCH7, were selected to identify $CD11b^{+}CD14^{-}CD15^{+}CD33^{+}HLADR^{-}$ cells and compare their frequency in BM samples from HAs vs MM patients using Infinicyt software (Cytognos SL, Salamanca, Spain). Screening of different granulocytic subsets in newly diagnosed patients enrolled in the PETHEMA/GEM2012MENOS65 study was performed with the following combination of mAbs: HLADR-PacB, CD45-OC515, CD36-FITC, CD13-PE, CD34-PerCPCy5.5, CD117-PECy7, CD11b-APC, and CD71-APCH7. EDTA-anticoagulated BM samples were processed within 24 hours after collection following the EuroFlow lyse-wash-and-stain standard sample preparation protocol, and data acquisition was performed in a FACSCanto II flow cytometer (Becton Dickinson/BD Biosciences, San Jose, CA) using FACSDiva 6.1 software (BD Biosciences). Flow cytometry standard files obtained from 55 patients studied in 1 of the 3 central laboratories of the Spanish Myeloma Group (Grupo Español de Mieloma/Programa para el Estudio de la Terapéutica en Hemopatías Malignas) were used as a discovery data set and analyzed with a semiautomated pipeline that performs batch analyses of flow cytometric data to avoid the variability intrinsic to manual analysis and reveals full cellular diversity based on unbiased clustering (described in detail in supplemental Methods). Briefly, this strategy allowed the systematic identification and quantification of a variable number of cell clusters, which were grouped according to the similarity of antigen expression profiles by using the bioinformatic algorithm FlowSOM (supplemental Figure 1).[17] After unbiased identification of cell clusters in the discovery data set, we performed manual analysis to quantify them in the remaining 212 patients enrolled in the PETHEMA/GEM2012MENOS65 clinical trial.

3-dimensional cultures

An organoid 3-dimensional model was developed to test the effect of daratumumab (10 μg/mL) on granulocytes from BM samples of MM patients (n = 3). Cells were lysed with 1X BulkLysis buffer (Cytognos), and 1×10^6 cells were embedded in 30 μL of Matrigel Matrix (Corning) and fibronectin (ratio of

matrigel/fibronectin, 2:1). This mix was seeded per well in a 48-well plate (Cellstar) and left for 40 minutes in the incubator so that the Matrigel solidified. Afterward, we added 300 μL of RPMI 1640 medium (10% fetal bovine serum, 1% L-glutamine, 1% Penicillin-Streptomycin) supplemented with 10% of plasma from the same BM sample, 100 nM of interleukin-6 (IL-6), and 100 nM of insulin-like growth factor-1 per well. Organoids were maintained in culture for 10 days at 37°C, and daratumumab (10 μg/mL) was added to the medium on days 1 and 5 of culture. Finally, organoids were desegregated with Cell Recovery Solution (Corning) and labeled with HLA-DR-BV421, CD45-OC515, CD16-FITC, CD13-PE, CD34-PerCP-Cy5.5, CD117-PE-Cy7, CD11b-APC, and CD10-APCH7. Data acquisition was performed in a FACSCanto II flow cytometer using FACSDiva software, and data analysis was performed using Infinicyt software. In addition, we analyzed the percentage of various granulocytic subsets present in BM samples from 36 MM patients collected before and after treatment with daratumumab, which were stained with the next-generation flow mAb panel designed to monitor plasma cell clonality (tube 1: CD138-BV421, CD27-BV510, CD38-FITC, CD56-PE, CD45-PerCPCy5.5, CD19-PECy7, CD117-APC, and CD81-APCH7; tube 2: CD138-BV421, CD27-BV510, CD38-FITC, CD56-PE, CD45-PerCPCy5.5, CD19-PECy7, cyKAPPA-APC, and cyLAMBDA-APCH7).[18] The first mAb combination of the next-generation flow panel was used to enumerate immature neutrophils ($CD38^{+}$, $CD45^{dim}$, $CD117^{+}$, SSC^{hi}), intermediate and mature neutrophils ($CD38^{-/lo}$, $CD45^{dim}$, $CD81^{-}$, $CD117^{-}$, SSC^{hi}), basophils ($CD38^{hi}$, $CD45^{dim}$, $CD81^{-}$, $CD117^{-}$, SSC^{lo}), and eosinophils ($CD38^{-/lo}$, $CD45^{bright}$, $CD81^{bright}$, $CD117^{-}$, SSC^{hi}).

Fluorescence-activated cell sorting

Cells with the preestablished G-MDSC phenotype ($CD11b^{+}CD14^{-}CD15^{+}CD33^{+}HLADR^{-}$) and 3 maturation stages of the neutrophil lineage were sorted from HAs (n = 15) and MM patients (n = 45) using a FACSAria II flow cytometer (BD Biosciences). Cells were stained with 7-AAD or Sytox Blue Dead to exclude dying events. Cells were stored in Lysis/Binding Buffer (Invitrogen, Carlsbad, CA) for RNA sequencing (RNAseq) or in phosphate-buffered saline plus 0.005% bovine serum albumin until processing for the assay for transposase-accessible chromatin with high-throughput sequencing (ATACseq) or used immediately for morphological assessment or functional assays. These are described in supplemental Methods.

RNAseq data from mesenchymal stem cells (MSCs) isolated by fluorescence-activated cell sorting from BM aspirates of age-matched HAs (n = 8) and MM patients (n = 56)[19] were used to compare the expression levels of genes coding for transforming growth factor β (TGF-β) and other soluble mediators potentially involved in the modulation of the BM tumor microenvironment.

Statistical analysis

The Kruskal-Wallis test was used to estimate the statistical significance observed between groups in T-cell immunosuppression assays. The Student *t* test was used to evaluate differences between groups in experiments measuring T-cell proliferation, as well as to evaluate significant associations between patients' clinical data and the distribution of various granulocytic subsets. Progression-free survival (PFS) was defined as the time from multidimensional flow cytometry assessment at diagnosis until disease progression or death resulting from any cause, estimated using the Kaplan-Meier method, and compared using a 2-sided stratified log-rank test. Patients were stratified into groups according to the median value of each cell type (or cell ratio) in the whole population. Statistical analyses were performed using GraphPad Prism software (version 7; San Diego, CA) and SPSS software (version 25.0.0; IBM, Chicago, IL). *P* values $<.05$ were considered statistically significant.

Results

Characterization of G-MDSCs based on conventional criteria

In humans, G-MDSCs have been previously defined as a unique (rare) population displaying a $CD11b^{+}CD14^{-}CD15^{+}CD33^{+}HLADR^{-}$ phenotype, comprising ~1% of BM nucleated cells in HAs and up to 25% in MM patients.[20] However, we found that the frequency of $CD11b^{+}CD14^{-}CD15^{+}CD33^{+}HLADR^{-}$ cells (gating strategy shown in supplemental Figure 2) among total BM nucleated cells was similar between HAs (n = 7) and MM patients (n = 10; median, 28% vs 24%, respectively; $P = .49$; Figure 1A). Moreover, rather than defining a unique population, $CD11b^{+}CD14^{-}CD15^{+}CD33^{+}HLADR^{-}$ cells included a mixture of neutrophil subsets (ie, metamyelocytes, band/mature neutrophils) plus eosinophils (supplemental Figure 2).

Because various granulocytic subsets were identified within putative G-MDSCs according to conventional phenotypic criteria, we decided to perform an unbiased analysis based on automated clustering using the antigens described above and others reported as potentially relevant[4] for MDSC isolation to reveal how many granulocytic clusters were present in BM samples from HAs and MM patients. This strategy led to the identification of eosinophils, basophils, and 3 well-defined neutrophil maturation stages according to differential expression of CD11b, CD13, and CD16 in HAs and MM patients: immature ($CD11b^{-}CD13^{-/lo}CD16^{-}$), intermediate ($CD11b^{+}CD13^{-/lo}CD16^{-}$), and mature ($CD11b^{+}CD13^{+}CD16^{+}$) neutrophils as confirmed by the expected shape of their nuclei (Figure 1B-C). Of note, the mean frequency of each of the 5 granulocytic subsets was similar between HAs and MM patients (Figure 1D), as was the percentage of each neutrophil subset within total neutrophils (data not shown). There were no differences in the phenotypic profile of mature neutrophils present in matched BM and PB samples from MM patients (n = 5), although as expected, immature and intermediate neutrophils were absent in PB (supplemental Figure 3A-B). On transcriptional grounds, mature neutrophils from BM and PB of MM patients clustered together and apart from those of HAs (supplemental Figure 3C).

Daratumumab has no long-term in vitro effect on BM granulocytes from MM patients

Based on previous data indicating that daratumumab depletes G-MDSCs,[11] we treated primary BM aspirates from MM patients (n = 3) with daratumumab to compare the number and phenotype of granulocytic cells before vs after treatment and thereby infer the antigen expression of putative G-MDSCs depleted by the drug. Samples were cultured in an organoid 3-dimensional model to enable long-term treatment (supplemental Figure 4A). As expected, daratumumab induced a significant depletion of tumor plasma cells (supplemental Figure 4B), but no differences were found regarding the percentage of $CD11b^{+}CD14^{-}CD15^{+}CD33^{+}HLADR^{-}$ cells (supplemental Figure 4C) or various granulocytic subsets (supplemental Figure 4D) after 10-day treatment with daratumumab. These results were confirmed ex vivo, where the percentage of various granulocytic subsets was

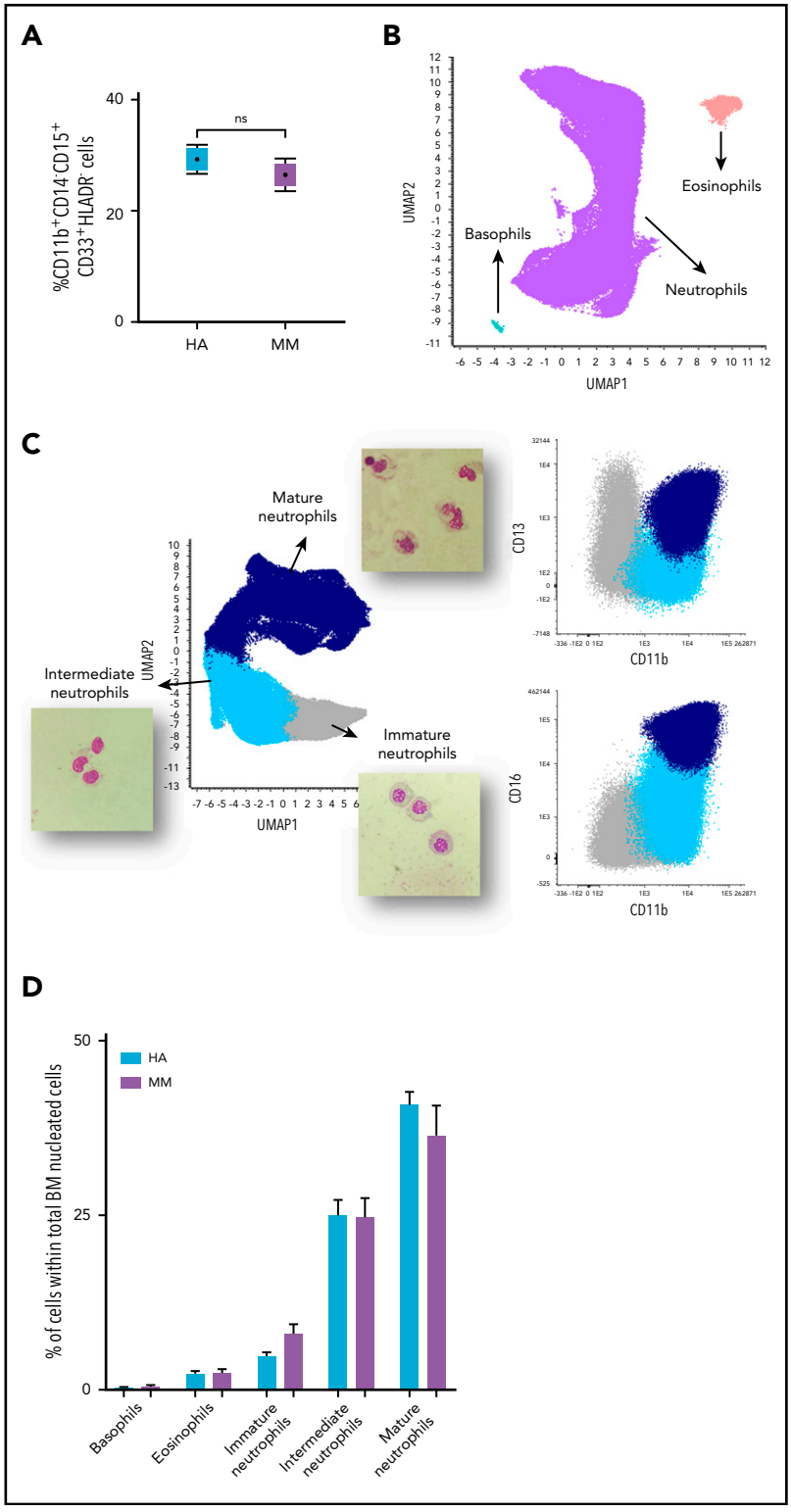

Figure 1. Characterization of G-MDSCs based on conventional criteria. (A) BM samples from MM patients (n = 10) and HAs (n = 7) were stained with HLADR-BV421, CD45-OC515, CD15-FITC, CD13-PE, CD33-PerCPCy5.5, CD16-PECy7, CD11b-APC, and CD14-APCH7 mAbs. Cells with a $CD11b^{+}CD14^{-}CD15^{+}CD33^{+}HLADR^{-}$ phenotype represent ~25% of total BM nucleated cells both in HAs and MM patients. (B) Unbiased analysis based on uniform manifold approximation and projection (UMAP) according to expression levels of HLADR, CD45, CD15, CD13, CD33, CD16, CD11b, and CD14 revealed various granulocytic subsets (neutrophils, eosinophils, and basophils) in BM samples from HAs and MM patients. (C) UMAP of the neutrophil population led to the identification of 3 neutrophil maturation stages according to differential expression of CD11b, CD13, and CD16: immature ($CD11b^{-}CD13^{-/lo}CD16^{-}$), intermediate ($CD11b^{+}CD13^{-/lo}CD16^{-}$), and mature ($CD11b^{+}CD13^{+}CD16^{+}$) neutrophils. Cellular maturation was confirmed on cytospinned cells from the 3 different populations by evidencing the classic changes in nuclear shape. Images are shown with a ×400 magnification. (D) Frequency of each granulocytic subset was similar between HAs and MM patients. Bars represent the mean and lines the standard deviation.

similar in paired BM samples from MM patients (n = 36) analyzed before and after treatment with daratumumab (supplemental Figure 4E).

Clinical significance of granulocytes in the tumor microenvironment

Because the preestablished phenotype of human G-MDSCs does not allow for the identification of a unique population of myeloid cells in the BM of HAs and MM patients (nor in different percentages), and because no myeloid cells were depleted by daratumumab in vitro to allow for identification of the phenotype of G-MDSCs, we sought to define their phenotypic profile based on the identification of granulocyte subsets of clinical significance in patients with newly diagnosed MM (n = 267). Overall, the frequency of basophils, eosinophils, and immature ($CD11b^{-}CD13^{-/lo}CD16^{-}$), intermediate ($CD11b^{+}CD13^{-/lo}CD16^{-}$), and

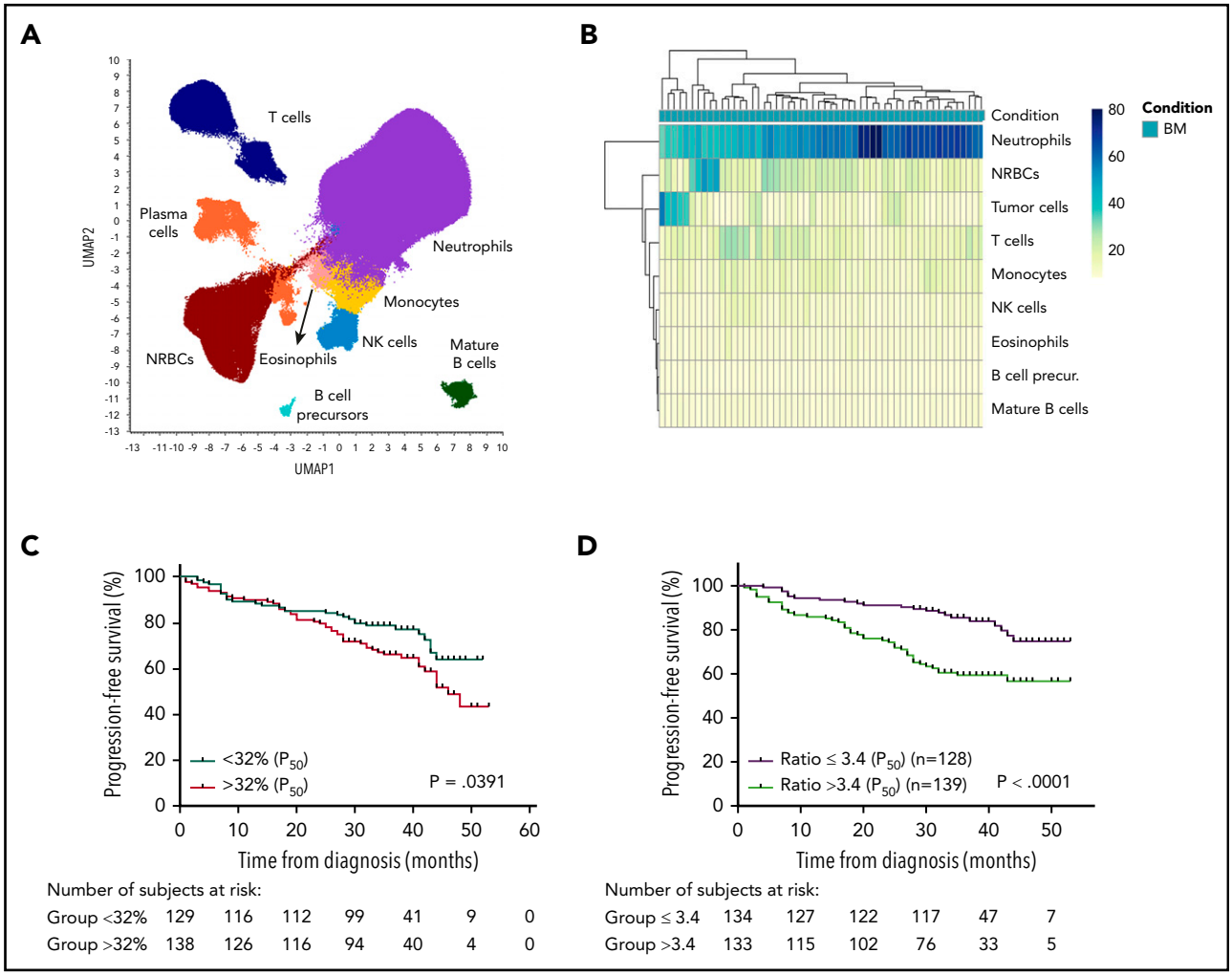

Figure 2. Clinical significance of granulocytes in the tumor microenvironment. (A) Unbiased immune monitoring of the tumor microenvironment based on uniform manifold approximation and projection (UMAP) of BM samples of newly diagnosed MM patients (n = 55). (B) Unsupervised clustering of MM patients based on cellular composition of the tumor microenvironment. (C) PFS according to high (>32%) vs low (≤32%) abundance of mature ($CD11b^+CD13^+CD16^+$) neutrophils (3-year PFS rate, 66% vs 79%, respectively; $P = .0391$). (D) PFS according to high (>3.4) vs low (≤3.4) mature neutrophil/T-lymphocyte ratio (3-year PFS rate, 60% vs 85%, respectively; $P < .0001$). NK, natural killer; NRBC, nucleated red blood cell.

mature ($CD11b^+CD13^+CD16^+$) neutrophils had no significant association with clinical parameters, including cytogenetic alterations (supplemental Figure 5A). However, we noted the presence of unique patient subgroups based on differential predominance of neutrophils, nucleated red blood cells, tumor cells, and T cells in the tumor microenvironment (Figure 2A-B). On prognostic grounds, we found that only the percentage of mature neutrophils and not any other granulocytic subset had a significant impact on PFS (supplemental Figure 5B); patients with >32% $CD11b^+CD13^+CD16^+$ BM cells had 3-year PFS rates of 66% vs 79% in cases with ≤32% mature neutrophils (Figure 2C). Because of the relationship between MDSCs and T-cell immunosuppression, we then explored if a mature neutrophil/T-lymphocyte ratio was prognostically relevant. Accordingly, patients with higher ratios (>3.4) had significantly inferior PFS when compared with cases with lower ratios (3-year PFS rate, 85% vs 60%, respectively; $P < .001$; Figure 2D).

Progressive immunosuppression from immature to mature neutrophils

As a result of the prognostic value found in regard to the frequency of mature neutrophils in the tumor microenvironment of MM patients, we then investigated the immunosuppressive potential of these cells with 2 functional assays: the proliferation rate of autologous T cells in the presence of CD3/CD28 stimulatory beads (n = 14; Figure 3A), and the cytotoxic potential of autologous T cells against MM cells using a BCMA×CD3-bispecific antibody (n = 10; Figure 3B). Interestingly, we noted a significant decrease in T-cell proliferation when these were stimulated in the presence of mature neutrophils from MM patients (0.5-fold; $P = .016$) but not from HAs (Figure 3C). By contrast, immature and intermediate neutrophil subsets from MM patients or HAs had no impact on T-cell proliferation. In addition, we noted that the cytotoxic potential of T cells engaged by a BCMA×CD3-bispecific antibody progressively increased with the depletion of immature, intermediate, and mature neutrophils (two-, three-, and fourfold, respectively; $P \leq .03$; Figure 3D).

Molecular characterization of neutrophil differentiation in normal and tumor BM

In light of the progressively increasing gradient of immunosuppression from immature to mature neutrophils, we decided

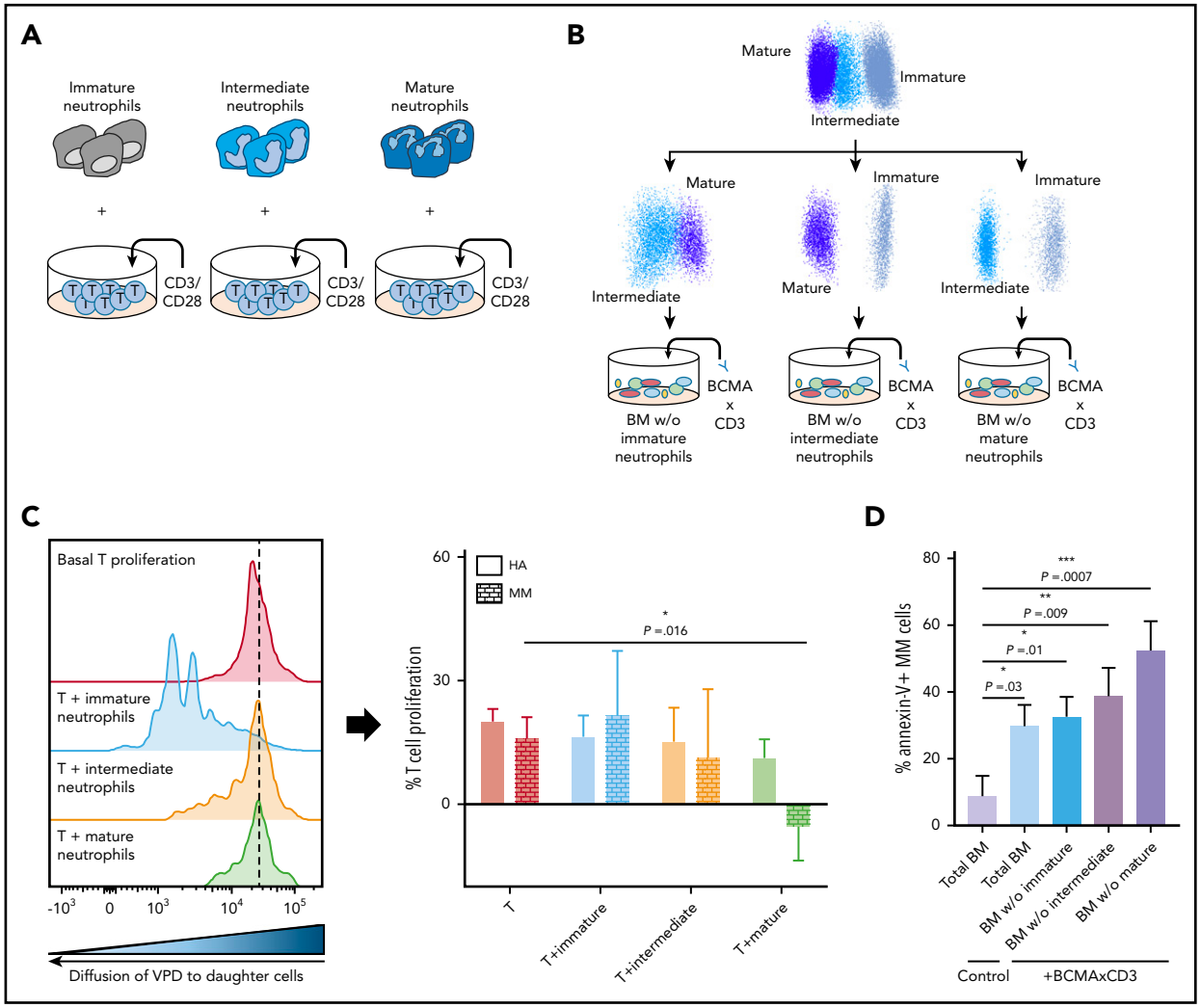

Figure 3. Progressive immunosuppression from immature to mature neutrophils. (A) Fluorescence-activated cell sorting of the 3 neutrophil subsets from BM samples of MM patients (n = 10) and HAs (n = 4) was performed to culture each subset with autologous T cells previously stimulated with CD3/CD28 antibodies and labeled with violet proliferation dye (VPD). After a 4-day incubation, VPD intensity was measured on total T cells. (B) Total BM samples vs BM samples depleted of each neutrophil subset (ie, BM without $CD11b^{-}CD13^{-/lo}CD16^{-}$, BM without $CD11b^{+}CD13^{-/lo}CD16^{-}$, and BM w/o $CD11b^{+}CD13^{+}CD16^{+}$) from MM patients (n = 10) were treated with 30 nM of a BCMA×CD3-bispecific antibody and left in culture for 24 hours. (C) Significant decrease in T-cell proliferation when these were stimulated in the presence of mature neutrophils from MM patients (0.5-fold; $P = .016$), but not the immature or intermediate subsets from MM patients or HAs. (D) Cytotoxic potential of T cells engaged by a BCMA×CD3-bispecific antibody progressively increased with the depletion of immature, intermediate, and mature neutrophils (two-, three-, and fourfold, respectively; $P \leq .03$). Bars represent the mean and lines the standard error of the mean. Statistical significance was evaluated using the Student *t* test for proliferation analysis and the Kruskal-Wallis test for the immunosuppression assay. $^{*}P < .05$, $^{**}P < .01$, $^{***}P < .001$.

to investigate if differences in the functional behavior of each neutrophil subset were related to transcriptional modulation after their differentiation. Unsupervised clustering after RNA-seq of immature, intermediate, and mature neutrophils from HAs and MM patients (n = 8 each) showed accurate segregation per cell type and not participant (Figure 4A), thereby validating CD11b, CD13, and CD16 as robust markers to identify and isolate neutrophil stages with different transcriptional profiles. Specific analysis of genes coding for cytokine/chemokine-soluble mediators based on the KEGG cytokine-cytokine receptor interaction pathway list (supplemental Table 1) revealed significantly different levels in 21 genes and various patterns of differential expression in immature, intermediate, and mature neutrophils (supplemental Figure 6A-B). Notably, most of these patterns were identical in HAs and MM patients, except for the *CXCL1*, *PTGS2*, *TGFB1*, *TNFSF13B*, *VEGFA*, *CCL4*, and *IL1B* genes, because their expression levels were significantly altered in mature neutrophils from MM patients (supplemental Figure 6C). Accordingly, unsupervised clustering at the subset level showed incomplete segregation between HAs and MM patients regarding the transcriptional profiles of immature and intermediate (supplemental Figure 7) but not mature neutrophils (Figure 4B), which segregated all HAs and MM patients based on differentially expressed genes. Interestingly, gene set enrichment analysis revealed that mature neutrophils from MM patients displayed reduced antiviral and anticancer type 1 and 2 interferon transcriptional response, as well as increased activation of transcriptional pathways related to inflammation, such as tumor necrosis factor α, IL-2–STAT5, and TGF-β signaling (Figure 4C).

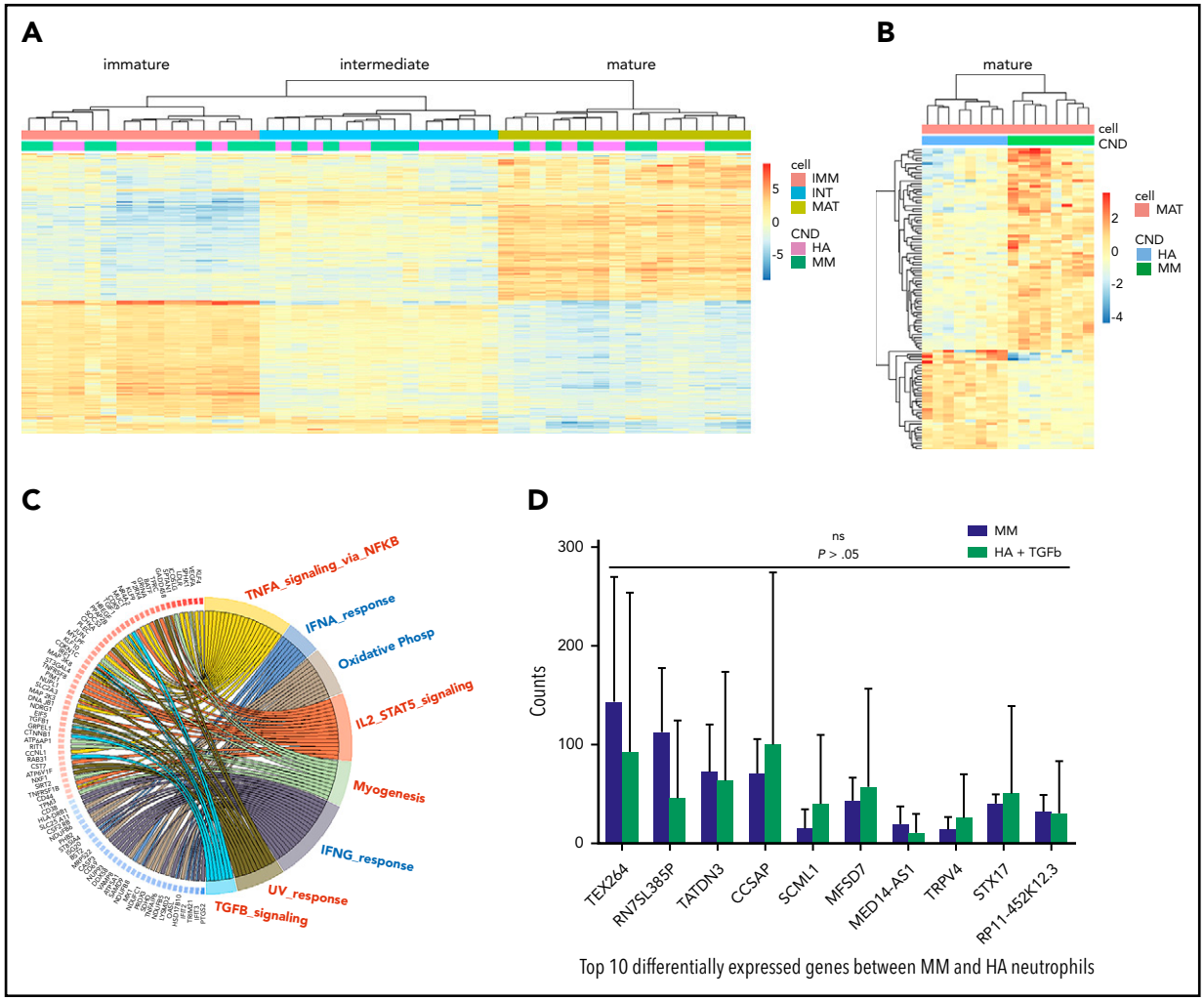

Figure 4. Molecular characterization of neutrophil differentiation in normal and tumor BM. (A) Unsupervised clustering after RNAseq of immature, intermediate, and mature neutrophils from HAs and MM patients (n = 8 each) showed accurate segregation per cell type and not participant. (B) Whole-transcriptome profiling through RNAseq segregates mature neutrophils from HAs and MM patients according to 108 genes differentially expressed ($P < .05$). (C) Gene set enrichment analysis showed that mature granulocytes from MM patients increased activation of pathways related to inflammation and reduced antiviral and anticancer type 1 and 2 interferon transcriptional response. (D) Mature neutrophils from HAs (n = 3) were treated with TGF-β, and expression levels of the top-10 differentially expressed genes between MM and HA neutrophils (panel B) were analyzed. There were no significant differences when we compared mature neutrophils from MM patients vs HAs treated with TGF-β ($P > .05$). CND, condition; ns, not significant; TNFA, tumor necrosis factor α.

TGF-β transcriptionally rewires mature neutrophils

Based on our transcriptomic findings and on the prominent role of TGF-β in the MM tumor microenvironment,[21,22] we exposed mature neutrophils from HAs (n = 3) to TGF-β and investigated if this cytokine could contribute to a shift in their transcriptional profile to a program similar to that found in mature neutrophils from MM patients. Therefore, we focused on the top-10 differentially expressed genes between mature neutrophils from HAs and MM patients identified above and compared their expression levels in MM patients vs mature neutrophils from HAs after treatment with TGF-β (Figure 4D). Accordingly, we found no significant differences ($P > .05$) in the expression of these genes, suggesting that TGF-β significantly contributes to the molecular reprogramming of mature neutrophils. Interestingly, MSCs from MM patients (n = 56) had similar expression levels of *TGF-β* as compared with those from age-matched HAs (n = 8), but genes coding for proinflammatory molecules (*CXCL2*, *CXCL3*, and *PTGS2*), growth factors (*IL-6*, *BAFF*), and angiogenetic mediators (*IL-8*), which eventually may also shift the transcriptome of mature neutrophils, were found to be upregulated in MSCs from MM patients (supplemental Figure 8).

Transcriptional network of mature neutrophils is epigenetically deregulated in MM

Under the hypothesis that the transcriptional changes found in mature neutrophils from MM patients resulted from epigenetic modulation as a consequence of the altered cellular and cytokine content in the tumor microenvironment, we integrated RNAseq data with chromatin accessibility profiling through ATACseq in mature neutrophils from BM aspirates of HAs (n = 3) and MM patients (n = 3). A mean of 23 214 open chromatin sites (peaks) in nucleosome-free regions in the 6 different samples was reported, and using a generalized linear model (DESeq2; adjusted $P < .1$), we identified 1445 differentially accessible peaks between mature neutrophils from HAs vs MM patients. Among these peaks, 678 showed an increase and 767 showed a decrease in chromatin accessibility in MM. To assess their

Table 1. Gene ontology enrichment analysis of genes closing or opening in mature neutrophils of MM patients vs HAs

ID	Description	*P*	Adjusted *P*
GO:0042119	Neutrophil activation	1.72e−11	3.56e−8
GO:0043312	Neutrophil degranulation	2.27e−11	3.56e−8
GO:0002283	Neutrophil activation involved in immune response	2.82e−11	3.56e−8
GO:0036230	Granulocyte activation	2.83e−11	3.56e−8
GO:0002446	Neutrophil-mediated immunity	6.15e−11	6.18e−8
GO:0031325	Positive regulation of cellular metabolic process	1.08e−10	8.60e−8
GO:0051173	Positive regulation of nitrogen compound metabolic process	1.20e−10	8.60e−8
GO:0009893	Positive regulation of metabolic process	3.33e−10	2.09e−7
GO:0043299	Leukocyte degranulation	5.13e−10	2.87e−7
GO:0002275	Myeloid cell activation involved in immune response	9.00e−10	4.29e−7

Several functions associated with closed regions predicted for altered neutrophil immunity in MM, while no functions were significantly associated with open regions.

biological relevance, differential peaks were annotated to the nearest gene based on their distance to transcription start sites (TSSs). Of note, 50% of these peaks were in potential promoter regions within 3 kb of a TSS, suggesting that these gains/losses in accessibility could exert regulatory activity (supplemental Figure 9A). Accordingly, we performed a gene ontology enrichment analysis on genes that were closing or opening in MM-derived mature neutrophils. Interestingly, we found several functions (the top 10 are described in Table 1) associated with closed regions that predicted for altered neutrophil immunity in MM, whereas no significant functions were found associated with open regions.

Based on paired ATACseq and RNAseq data, we found a significant correlation between gains or losses of chromatin accessibility near TSSs and gene expression for each normal and tumor-derived neutrophil sample (supplemental Figure 9B). To confirm these results, we selected *CD83*, which showed significantly higher messenger RNA expression in MM patients vs HAs, as well as concordant transcriptional and chromatin accessibility data, and confirmed its increased protein expression in MM by flow cytometry (supplemental Figure 9C). Most importantly, we observed a significant positive correlation between MM-specific changes in gene expression levels and chromatin accessibility at gene promoters in mature neutrophils ($P = 8.17e^{-6}$; Figure 5A). Furthermore, gene ontology enrichment analysis of differentially expressed genes in mature neutrophils from MM patients revealed a significant downregulation in functions related to neutrophil immune activation, in accordance with chromatin accessibility (Figure 5B).

These results led us to investigate if DNA demethylation induced by CM-272, a selective and reversible inhibitor of histone methyltransferase G9a and DNA methyltransferase,[23] could open chromatin regions that were closed in mature neutrophils from MM patients and reinduce expression of genes related to neutrophil immune activation. Accordingly, we found dose-dependent transcriptional changes in mature neutrophils from MM patients after treatment with CM-272 (Figure 5C) and validated their mode of action by confirming increased expression of several type 1 interferon–related genes (supplemental Figure 10).[23] Most importantly, we observed a significant enrichment of upregulated genes related with neutrophil activation (Figure 5D), which suggests that hypomethylating agents could potentially be used to revert the immunosuppressive signature of mature neutrophils present in the tumor microenvironment. Accordingly, we noted that the cytotoxic potential of T cells engaged by a BCMA×CD3-bispecific antibody was restored and even enhanced when mature neutrophils were pretreated with CM-272 (supplemental Figure 11).

Discussion

Emerging immunotherapies have shown efficacy in the treatment of early- and late-stage MM.[24-26] Therefore, better understanding of the complexity and diversity of the tumor immune milieu is warranted to improve the ability to predict, monitor, and guide immunotherapeutic responsiveness. By integrating the clinical significance with the immunosuppressive potential and molecular network of various granulocytic subsets in the BM, we provide for the first time a set of markers for optimal monitoring of G-MDSCs in MM.

There is growing interest in targeting immunosuppressive cells to optimize T-cell activity and immunotherapy efficacy in MM. However, the ability to specifically target immunosuppressive cells while preserving the function of antitumor immune cells remains a challenge in the absence of specific cell markers, and MDSCs are a good example of this conundrum. MDSCs were first described in 2007,[27] but since then, the few studies performed in humans have commonly required isolation by density centrifugation of PB samples because of the lack of markers to isolate G-MDSCs from other cells in the tumor microenvironment.[4] Interestingly, these low-density granulocytes were found to be a heterogeneous mix of both banded and segmented neutrophils,[4,28] but not of more immature stages. These findings are consistent with the observation made in this study that there is a gradient of progressive immunosuppression from immature to mature neutrophils, reaching its maximum at the banded/segmented stage.

The G-MDSC–specific Gr-1 surface antigen is only present in mice, and therefore, human G-MDSCs have been attributed to a broader $CD11b^{+}CD14^{-}CD15^{+}CD33^{+}HLADR^{-}$ phenotype. However, we showed that this combination of markers could not distinguish G-MDSCs from common neutrophils; in fact, most maturing granulocytes are $CD11b^{+}$, CD15 is also expressed in eosinophils, and CD33 is present in all myeloid cells. CD16 has been proposed as an additional marker[29] to identify G-MDSCs, but alone it is not

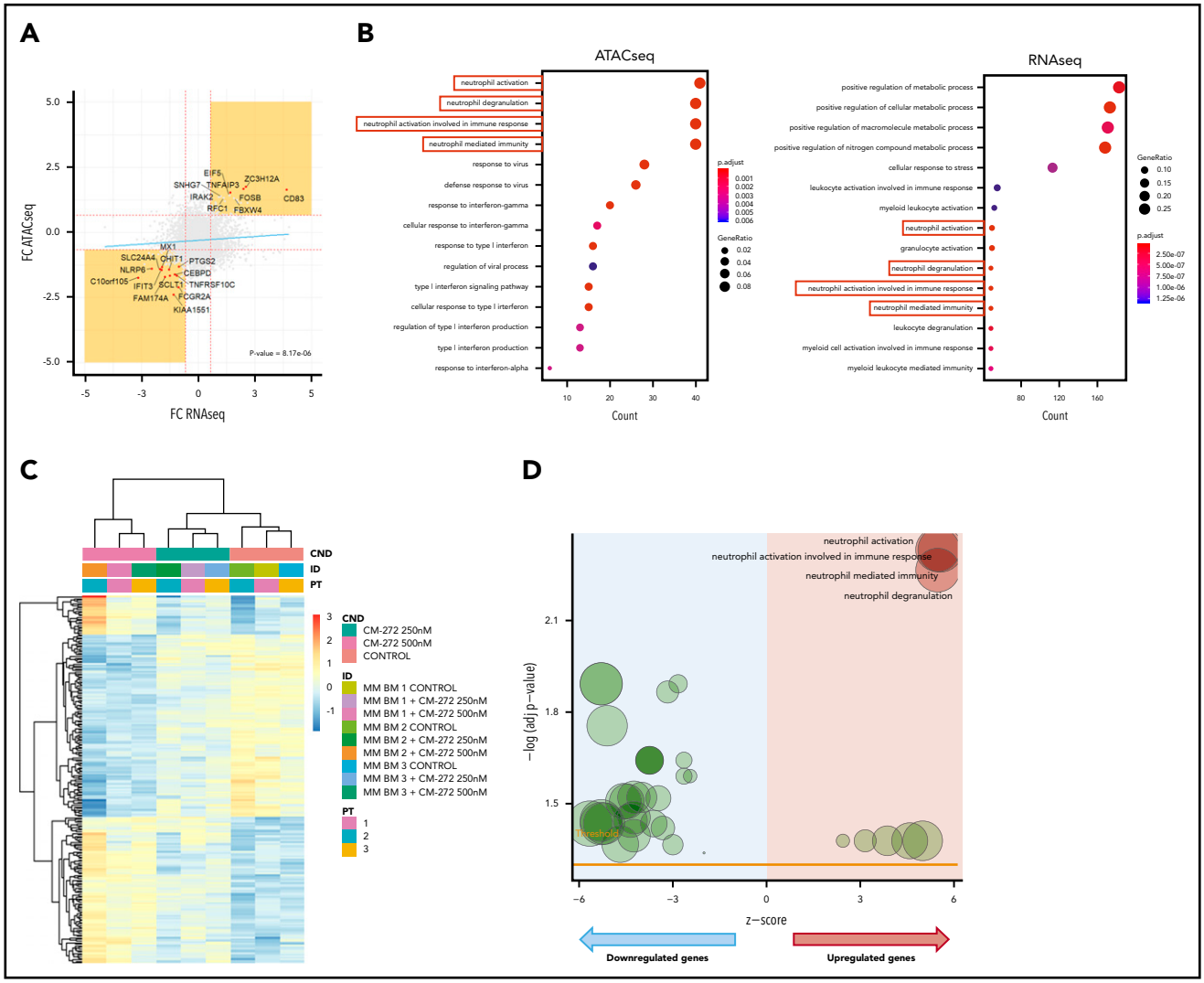

Figure 5. Transcriptional network of mature neutrophils is epigenetically deregulated in MM. (A) Correlation between gains and losses of chromatin accessibility near TSSs and gene expression for each sample. Significant positive correlation between MM-induced changes in gene expression level and chromatin accessibility at gene promoters in mature granulocytes ($P = 8.17e^{-6}$). (B) Gene ontology enrichment analysis of differentially expressed genes underscores functions related to neutrophil activation in MM. (C) Transcriptional analysis of mature neutrophils from MM patients (n = 3) treated with CM-272–segregated samples according to exposure and concentration of the drug. (D) Gene ontology enrichment analysis based on upregulated genes in mature neutrophils from MM patients after treatment with CM-272. FC, fold-change.

sufficient, because it is also expressed in nonclassic monocytes that coincidently downregulate CD14.[30] Therefore, in the absence of established markers, human G-MDSCs can only be defined by their functional hallmarks (T-cell suppression and arginase 1 expression). We show that mature neutrophils (and no other granulocytic subset) present in the MM tumor microenvironment correlate with patient outcome. Furthermore, these cells exerted the strongest T-cell immunosuppression and expressed higher levels of inflammatory cytokines, such as *TGFB1*, *TNF*, and *VEGFA*, together with an increase in NF-κB and other G-MDSC-associated markers (eg, *PTGS2*, *CSF1*, *IL-8*, *IRF1*, *IL4R*, *STAT1*, *STAT3*, *STAT6*) when compared with intermediate and immature neutrophils.[31-33] Therefore, we propose that in MM, G-MDSCs are $CD11b^{+}CD13^{+}CD16^{+}$ neutrophils.

Structured models of transcriptional, phenotypic, and functional diversity are instrumental for better understanding of immune cell biology. However, unlike in other myeloid cells, in which diverse functional properties have been linked to specific molecular programs, the transcriptional heterogeneity behind the functional diversity of neutrophils remains largely unknown.[34] Here, after identifying surface markers enabling the tracking of immunosuppressive neutrophils (ie, G-MDSCs) within the MM tumor microenvironment, we show that maturing neutrophil subsets have unique gene expression profiles that are rewired into an immunosuppressive state through epigenetic modulation in the BM of patients with cancer. It has been suggested that TGF-β, an immunosuppressive cytokine produced by tumor cells from various cancer types, polarizes neutrophils to a protumorigenic phenotype.[35,36] Here, we show that exposure to TGF-β is able to shift the transcriptional profile of mature neutrophils from HAs to a program similar to that found in MM, and future studies are warranted to investigate a possible correlation between TGF-β level and the immunosuppressive potential of G-MDSCs in BM aspirates. Additional research should also be performed to identify which other players in the BM milieu may contribute to this phenomenon. Finally, we show that the molecular network of

mature neutrophils from MM patients could be modified by epigenetic drugs and thereby prevent their immunosuppressive effect in T cells engaged by a BCMA×CD3-bispecific antibody. Therefore, this study proposes further investigation of their biology to identify targeted therapies for the rewiring of G-MDSCs and increase the successful application of immunotherapy in MM and other tumors.

Acknowledgments

This study was supported by the Centro de Investigación Biomédica en Red–Área de Oncología–del Instituto de Salud Carlos III (CB16/12/00369, CB16/12/00489, CB16/12/00233, and CB16/12/00400); Instituto de Salud Carlos III/Subdirección General de Investigación Sanitaria (FIS #PI17/01243); Fondo Europeo de Desarrollo Regional; and Asociación Española Contra el Cáncer (FCAECC; Predoctoral Grant Junta Provincial Navarra). This study was also supported internationally by Cancer Research UK, FCAECC, and Associazione Italiana per la Ricerca sul Cancro under the Accelerator Award Programme; the Black Swan Research Initiative of the International Myeloma Foundation; the European Research Council 2015 Starting Grant (MYELOMANEXT); the Multiple Myeloma Research Foundation Immunotherapy Networks of Excellence; and a 2017 European Hematology Association nonclinical advanced research grant (#3680644).

Authorship

Contribution: C.P., C.B., and B.P. conceived of the idea and designed the study protocol; C.P. and C.B. analyzed flow cytometric data; D. Alignani performed cell sorting; C.P. performed in vitro experiments; C.P., S.S., and A.V.-Z. performed next-generation sequencing; C.B. and I.G. analyzed sequencing data; A.Z., N.P., E.S.J.-E., J. Merino, P.R.-O., C.M., P.M., I.M., D.L.-A., C.R., M.R., M.-J.B., R.R., J. Martin, J.B., J.d.l.R., X.A., M.-T.C., J.M.-L., C.B., F.P., A. Orfao, A. Oriol, A.S., M.-T.H., R.M., L.R., M.-V.M, J.-J.L., J.B., and J.F.S.-M. provided study material and/or patients; C.P. and C.B. performed statistical analysis; C.P., C.B. and B.P. wrote the manuscript; and all authors reviewed and approved the manuscript.

Conflict-of-interest disclosure: A. Oriol participated in advisory boards for Amgen, Celgene and Janssen. M.-V.M. has received honoraria for lectures from or participated in advisory boards for Janssen, Celgene, Amgen, Takeda, AbbVie, Adaptive, GSK, Pharmamar, EDO, and Oncopeptides. L.R. reports honoraria from Janssen, Celgene, Amgen, and Takeda. J.B. reports honoraria for lectures from Janssen, Amgen, Celgene, Takeda, and Oncopeptides. J.-J.L. reports honoraria from and membership on boards of directors or advisory committees with Takeda, Amgen, Celgene, and Janssen. J.F.S.-M. reports consultancy for Bristol-Myers Squibb, Celgene, Novartis, Takeda, Amgen, MSD, Janssen, and Sanofi and membership on a board of directors or advisory committee with Takeda. B.P. reports honoraria for lectures from and membership on advisory boards with Amgen, Bristol-Myers Squibb, Celgene, Janssen, Merck, Novartis, Roche, and Sanofi; unrestricted grants from Celgene, EngMab, Sanofi, and Takeda; and consultancy for Celgene, Janssen, Sanofi, and Takeda. The remaining authors declare no competing financial interests.

A complete list of the members of the Grupo Español de Mieloma/Programa para el Estudio de la Terapéutica en Hemopatías Malignas appears in "Appendix."

ORCID profiles: C.B., 0000-0002-1522-4504; I.G., 0000-0002-5329-2225; D. Alameda, 0000-0002-6598-7163; E.S.J.-E., 0000-0001-5786-5273; A.V.-Z., 0000-0001-6693-0989; A. Oriol, 0000-0001-6804-2221; Rafael Rios, 0000-0001-8193-1402; J.d.l.R., 0000-0002-8354-768X; M.-T.H., 0000-0002-6576-7881; F.P., 0000-0001-6115-8790; J.-J.L., 0000-0002-3393-9570; J.F.S.-M., 0000-0002-9183-4857.

Correspondence: Bruno Paiva, Clínica Universidad de Navarra, Centro de Investigación Médica Aplicada (CIMA), Av. Pío XII 55, 31008, Pamplona, Spain; e-mail: bpaiva@unav.es.

Footnotes

Submitted 20 December 2019; accepted 3 April 2020; prepublished online on *Blood* First Edition 23 April 2020. DOI 10.1182/blood.2019004537.

*C.P. and C.B. contributed equally to this study as first authors.

The sequencing data reported in this article have been deposited in the Gene Expression Omnibus database (accession number GSE150023).

For original data, please e-mail the corresponding author.

The online version of this article contains a data supplement.

The publication costs of this article were defrayed in part by page charge payment. Therefore, and solely to indicate this fact, this article is hereby marked "advertisement" in accordance with 18 USC section 1734.

Appendix

The members of the Grupo Español de Mieloma/Programa para el Estudio de la Terapéutica en Hemopatías Malignas Cooperative Study Group are: María Casanova Espinosa, José Luís Guzman Zamudio, Eduardo Ríos Herranz, Rafael Rios Tamayo, Jesús Martín Sánchez, Luís Palomera Bernal, Ana Pilar González Rodríguez, María Esther González García, Antonia Sampol Mayol, Joan Bargay Lleonart, Alexia Suárez, Miguel Teodoro Hernández García, Carmen Montes Gaisán, Belén Hernández Ruiz, Felipe Casado Montero, Dunia de Miguel Llorente, Fernando Solano Ramos, Ángela Ibañez Garcia, Mariví Mateos Manteca, José Mariano Hernández Martín, Fernando Escalante Barrigón, Javier García Frade, Alfonso García de Coca, Carlos Aguilar Franco, Jorge Labrador Gómez, Elena Cabezudo Pérez, Joan Bladé Creixentí, Ana María Sureda Balari, Yolanda González Montes, Lourdes Escoda Teigell, Antonio García Guiñón, Eugenia Abella Monreal, Juan Alfonso Soler Campos, Josep María Martí Tutusaus, Albert Oriol Rocafiguera, Miquel Granell Gorrochategui, Mercedes Gironella Mesa, Carmen Cabrera Silva, Marta Sonia González Pérez, Ana Dios Loureiro, José Angel Méndez Sánchez, María Josefa Nájera Irazu, Francisco Javier Peñalver Párraga, Juan José Lahuerta Palacios, Pilar Bravo Barahona, Cristina Encinas Rodríguez, José Ángel Hernández Rivas, Jaime Pérez de Oteyza, Rebeca Iglesias del Barrio, Ana López de la Guia, Adrián Alegre Amor, Elena Prieto Pareja, Isabel Krsnik Castelló, María Jesús Blanchard Rodríguez, Rafael Martínez Martínez, Rosalía Riaza Grau, Eugenio Giménez Mesa, Elena Ruiz Sainz, Felipe de Arriba, Jose María Moraleda Jiménez, Marta Romera, Felipe Prósper Cardoso, José María Arguiñano Pérez, María Puente Pomposo, Ernesto Pérez Persona, Ana Isabel Teruel Casasús, Paz Ribas García, Isidro Jarque Ramos, María Blanca Villarrubia Lor, Pedro Luis Fernández García, Carmen Martínez Chamorro.

REFERENCES

1. Gabrilovich DI, Ostrand-Rosenberg S, Bronte V. Coordinated regulation of myeloid cells by tumours. *Nat Rev Immunol*. 2012;12(4):253-268.
2. Botta C, Gullà A, Correale P, Tagliaferri P, Tassone P. Myeloid-derived suppressor cells in multiple myeloma: pre-clinical research and translational opportunities. *Front Oncol*. 2014;4:348.
3. Gabrilovich DI, Nagaraj S. Myeloid-derived suppressor cells as regulators of the immune system. *Nat Rev Immunol*. 2009;9(3):162-174.
4. Giese MA, Hind LE, Huttenlocher A. Neutrophil plasticity in the tumor microenvironment. *Blood*. 2019;133(20):2159-2167.
5. Bronte V, Brandau S, Chen SH, et al. Recommendations for myeloid-derived suppressor cell nomenclature and characterization standards. *Nat Commun*. 2016;7:12150.
6. Greten TF, Manns MP, Korangy F. Myeloid derived suppressor cells in human diseases. *Int Immunopharmacol*. 2011;11(7):802-807.
7. De Veirman K, Van Valckenborgh E, Lahmar Q, et al. Myeloid-derived suppressor cells as therapeutic target in hematological malignancies. *Front Oncol*. 2014;4:349.

8. Malek E, de Lima M, Letterio JJ, et al. Myeloid-derived suppressor cells: the green light for myeloma immune escape. *Blood Rev*. 2016; 30(5):341-348.

9. Ramachandran IR, Martner A, Pisklakova A, et al. Myeloid-derived suppressor cells regulate growth of multiple myeloma by inhibiting T cells in bone marrow. *J Immunol*. 2013; 190(7):3815-3823.

10. Tadmor T. The growing link between multiple myeloma and myeloid derived suppressor cells. *Leuk Lymphoma*. 2014;55(12): 2681-2682.

11. Krejcik J, Casneuf T, Nijhof IS, et al. Daratumumab depletes CD38+ immune regulatory cells, promotes T-cell expansion, and skews T-cell repertoire in multiple myeloma. *Blood*. 2016;128(3):384-394.

12. De Veirman K, Menu E, Maes K, et al. Myeloid-derived suppressor cells induce multiple myeloma cell survival by activating the AMPK pathway. *Cancer Lett*. 2019;442:233-241.

13. Wang J, De Veirman K, De Beule N, et al. The bone marrow microenvironment enhances multiple myeloma progression by exosome-mediated activation of myeloid-derived suppressor cells. *Oncotarget*. 2015;6(41): 43992-44004.

14. Rosiñol L, Oriol A, Rios R, et al. Bortezomib, lenalidomide, and dexamethasone as induction therapy prior to autologous transplant in multiple myeloma. *Blood*. 2019;134(16): 1337-1345.

15. Paiva B, Puig N, Cedena MT, et al; GEM (Grupo Español de Mieloma)/PETHEMA (Programa Para el Estudio de la Terapéutica en Hemopatías Malignas) Cooperative Study Group. Measurable residual disease by next-generation flow cytometry in multiple myeloma. *J Clin Oncol*. 2019;38(8): 784-792.

16. Chesney JA, Mitchell RA, Yaddanapudi K. Myeloid-derived suppressor cells-a new therapeutic target to overcome resistance to cancer immunotherapy. *J Leukoc Biol*. 2017; 102(3):727-740.

17. Van Gassen S, Callebaut B, Van Helden MJ, et al. FlowSOM: using self-organizing maps for visualization and interpretation of cytometry data. *Cytometry A*. 2015;87(7): 636-645.

18. Flores-Montero J, Sanoja-Flores L, Paiva B, et al. Next generation flow for highly sensitive and standardized detection of minimal residual disease in multiple myeloma. *Leukemia*. 2017;31(10):2094-2103.

19. Alameda D, Saez B, Lara-Astiaso D, et al. Characterization of freshly isolated mesenchymal stromal cells from healthy and multiple myeloma bone marrow: transcriptional modulation of the microenvironment [published online ahead of print 23 January 2020]. *Haematologica*. doi:10.3324/haematol.2019.235135.

20. Görgün GT, Whitehill G, Anderson JL, et al. Tumor-promoting immune-suppressive myeloid-derived suppressor cells in the multiple myeloma microenvironment in humans. *Blood*. 2013;121(15):2975-2987.

21. Frassanito MA, De Veirman K, Desantis V, et al. Halting pro-survival autophagy by TGFβ inhibition in bone marrow fibroblasts overcomes bortezomib resistance in multiple myeloma patients. *Leukemia*. 2016;30(3): 640-648.

22. Lu A, Pallero MA, Lei W, et al. Inhibition of transforming growth factor-β activation diminishes tumor progression and osteolytic bone disease in mouse models of multiple myeloma. *Am J Pathol*. 2016;186(3):678-690.

23. San José-Enériz E, Agirre X, Rabal O, et al. Discovery of first-in-class reversible dual small molecule inhibitors against G9a and DNMTs in hematological malignancies. *Nat Commun*. 2017;8:15424.

24. Facon T, Kumar S, Plesner T, et al; MAIA Trial Investigators. Daratumumab plus lenalidomide and dexamethasone for untreated myeloma. *N Engl J Med*. 2019;380(22): 2104-2115.

25. Mateos MV, Hernández MT, Giraldo P, et al. Lenalidomide plus dexamethasone for high-risk smoldering multiple myeloma. *N Engl J Med*. 2013;369(5):438-447.

26. Raje N, Berdeja J, Lin Y, et al. Anti-BCMA CAR T-cell therapy bb2121 in relapsed or refractory multiple myeloma. *N Engl J Med*. 2019; 380(18):1726-1737.

27. Gabrilovich DI, Bronte V, Chen SH, et al. The terminology issue for myeloid-derived suppressor cells. *Cancer Res*. 2007;67(1):425, author reply 426.

28. Sagiv JY, Michaeli J, Assi S, et al. Phenotypic diversity and plasticity in circulating neutrophil subpopulations in cancer. *Cell Rep*. 2015; 10(4):562-573.

29. Pillay J, Tak T, Kamp VM, Koenderman L. Immune suppression by neutrophils and granulocytic myeloid-derived suppressor cells: similarities and differences. *Cell Mol Life Sci*. 2013;70(20):3813-3827.

30. Damasceno D, Andrés MP, van den Bossche WB, et al. Expression profile of novel cell surface molecules on different subsets of human peripheral blood antigen-presenting cells. *Clin Transl Immunology*. 2016;5(9):e100.

31. Condamine T, Mastio J, Gabrilovich DI. Transcriptional regulation of myeloid-derived suppressor cells. *J Leukoc Biol*. 2015;98(6): 913-922.

32. Fan C, Stendahl U, Stjernberg N, Beckman L. Association between orosomucoid types and cancer. *Oncology*. 1995;52(6):498-500.

33. Yuan M, Zhu H, Xu J, Zheng Y, Cao X, Liu Q. Tumor-derived CXCL1 promotes lung cancer growth via recruitment of tumor-associated neutrophils. *J Immunol Res*. 2016;2016: 6530410.

34. Ng LG, Ostuni R, Hidalgo A. Heterogeneity of neutrophils. *Nat Rev Immunol*. 2019;19(4): 255-265.

35. Andzinski L, Kasnitz N, Stahnke S, et al. Type I IFNs induce anti-tumor polarization of tumor associated neutrophils in mice and human. *Int J Cancer*. 2016;138(8):1982-1993.

36. Pylaeva E, Lang S, Jablonska J. The essential role of type I interferons in differentiation and activation of tumor-associated neutrophils. *Front Immunol*. 2016;7:629.